IJCRT.ORG ISSN : 2320-2882

INTERNATIONAL JOURNAL OF CREATIVE RESEARCH THOUGHTS (IJCRT)

An International Open Access, Peer-reviewed, Refereed Journal

Microstructural and optical properties of Ni-doped Fe_2O_3 nanoparticles prepared via Sol Gel Method

Jyoti Yadav*, Rimpy Shukla

DEPARTMENT OF PHYSICS, IIS(deemed to be UNIVERSITY), JAIPUR

Abstract: In this investigation, Hematite Fe_2O_3 and Ni doped Fe_2O_3 have been synthesized by simple chemical method sol gel process. Effect of different concentration of Ni doped Fe_2O_3 shows change the size, morphology, optical bandgap. The samples were Characterized by X-ray diffraction (XRD), Scanning electron Microscope (SEM), Fourier transform Infrared Spectroscopy (FTIR), UV-Visible Spectroscopy (UV-Vis). All the technique confirms the sample formation of pure and doped hematite phase. when the nickel concentration increased up to 20 % the doped nanoparticles showed an optical band gap decrease from 2.4 to 1.8 eV.

Keywords: Fe_2O_3, Composite, XRD, UV-Vis

1. Introduction

The most versatile metal oxide nanostructure groups of semiconductor nanostructures stand out as one of the most diverse and most probably richest class of materials due to their extensive structural, physical and chemical properties and functionalities. In this times metal oxides have been at the heart of many dramatic advances in the materials science. The Ferous oxide has four crystallographic phases, namely hematite (α-Fe_2O_3) antiferromagnetic, maghemite (γ-Fe_2O_3) ferromagnetic, β-Fe_2O_3 and ε-Fe_2O_3 .The thermodynamics stable hematite phase of Fe_2O_3 is an functional semiconductor (Eg =2.1 eV) which is environmentally friendly, nontoxic and important in various field. It has been the widely investigated material due to its various applications in the field of photocatalyst , pigments, gas sensors, solar cells , electrochemical sensor and lithium ion batteries etc. Since the structural and crystallographic forms are generally responsible for their properties, many methods for the synthesis of Fe_2O_3 including hydrothermal synthesis, forced hydrolysis , combustion method, microwave irradiation method, spray pyrolysis, chemical vapor deposition, pulsed laser deposition, co-precipitation and high vacuum evaporation and sol-gel is mainly interesting method due to its low cost, high purity, short preparation time, homogeneous solution of doping element and magnify the excellent polycrystalline samples. By doping of different metal oxides or any composite ion it will amplify to find new application and improve the performance of any other applications. The transition metals, nickel (Ni) has been analysed because Ni doping can increase the absorption range and morphogical change of Fe_2O_3 . Ni^{2+} ion involves absorption of atoms or ions into host lattices (Fe^{3+}) to yield composite materials with desirable properties and functions.

In my work we use the sol-gel process to prepare Ni doped in Fe_2O_3 nanoparticles from ferric nitrate and Nickel nitrate and triethaloamine. To find out the structural, morphological, Chemical bonds and optical properties are studied by XRD, SEM, FTIR and UV-Visible Spectroscopy to prepare the nanoparticles of Nickel doped iron oxides which depend on concentrations of the nickel by wt%.

2. Experimental Methods

2.1 Material

All reagents used in the synthesis used without any purification Iron nitrate and nickel nitrate was as precursor and triethaloamine were used in the solution while ammonia hydroxide (NH_4OH) was the precipitating agent, and double distilled water as solvent was used for the solution and washing they were obtained from Fisher Scientific corporation.

2.2 Sample Preparation

In this procedure, the aqueous solution of appropriate amount of iron nitrate and nickel nitrate were dissolved in 150 ml of deioinzed distilled water. The mole ratio by wt% of Ni and Fe was 10:90, 15:85 and 20:80. The mixture was allowed for magnetic stirring for 2 h. Ammonia hydroxide (NH_4OH) was used to adjust the pH to 10. Dark raddish colour prepared solution were filtered and washed several time with water and ethanol. Then it was dried at 110^0C in oven. The formed gel was calcined at 500^0C and it turns black in colour.

2.3 Characterization

The X-ray diffraction patterns of the samples were Using Bruker, Model D8 Advance with CuKα radiation (1.5418 Å) as a source. The intensity of peaks were collected over the range of 20°–80°. Fourier Transform Infrared pattern of the samples were using Perkin Elmer Spectrum in the range of 500-4000 cm^{-1} .UV-Vis pattern of the samples were using PerkinElmer UV WinLab in the range of 200-800 nm. To find Surface morphology Scanning electron Microscope were recorded in MIRA3 TESCAN.

3. RESULTS AND DISCUSSIONS

3.1 XRD Analysis

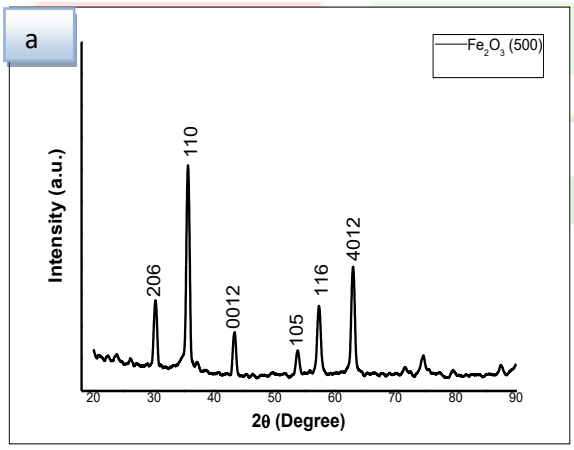

Fig.1(a) Pure Fe_2O_3at temp.500ºC

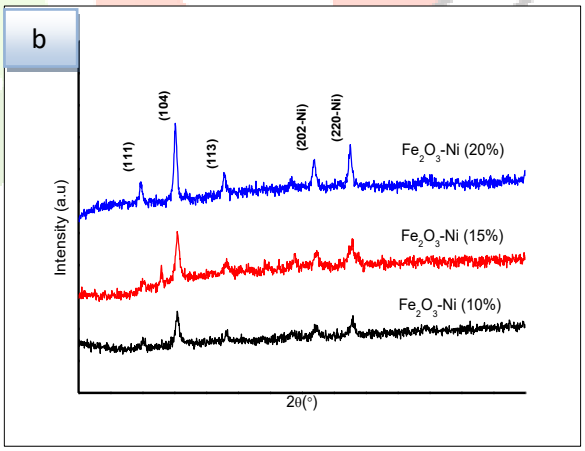

Fig.1(b)Comparsion of Fe_2O_3-Ni with different concentration

Fig.1(b) Shows XRD pattern of powder Ni doping in different concentrations (from 10 to 20%) in Fe_2O_3 with observed 2θ peaks lying at 2θ=29.7º (111), 2θ=35.1º (104), 2θ=42.8º (113), 2θ=56.7º (202-Ni) and 2θ=62.5º (220-Ni). All the observed peaks of spectra are indexed to the orthorhombic structue with space group R-3c and hematite matrix without changing the structure of Fe_2O_3 with the doping concentration. Which is good agreement with the literature (PDF no. 33-0664, 652901). No extra peaks associated with nickel oxide or phases of iron oxide were observed in range studied. Morever, the intensity of peaks (104) and (220) are increased gradually with the Ni-doping content. This is in agreement with the increase of half height width of the diffraction peaks and grain size. However, by increasing nickel concentration the peaks width is also increases and grain size is decrease.

The average crystallite size (D) of nanoparticles was obtained by Debye-Scherrer's formula given by equation

$$D=K\lambda/(\beta\cos\theta)$$

Where, D is the crystal size; λ is the wavelength of the X-ray radiation (λ=0.15409 nm) for CuKα. The average size of NiO nanostructure in XR patterns was 12nm which is attributed to the material nanoscale size. On the basis of Scherrer's equation, by increasing the concentration of Ni crystalline size of doped Fe_2O_3 decreases.

3.2 FT-IR Analysis

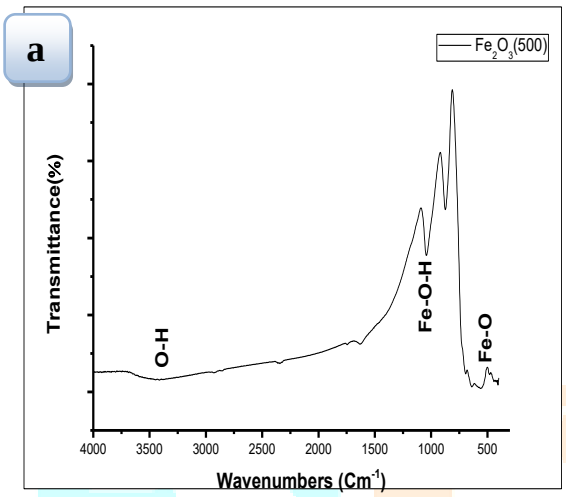

Fig.2(a) Pure Fe_2O_3at temp.500ºC

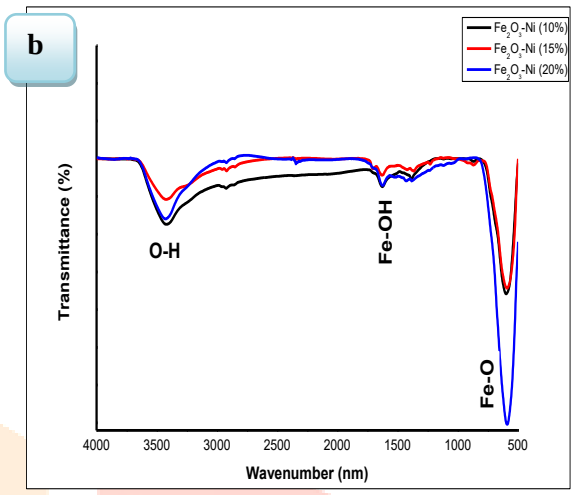

Fig.2(b) Comparsion of Fe_2O_3-Ni with different concentration

FT-IR spectroscopy was used to detect the presence of functional groups absorbed on the surface of synthesized particles by sol gel process. Figure 2(b) represents the FT-IR spectra of Ni doped Fe_2O_3 with different calcined at 500 °C.

The characteristic bands at 3402, 1626, 566, and 445 cm^{-1} were observed . The absorption band assigned with the water molecule of stretching and bending vibration is observed in a region of 3402 cm^{-1} and 1626 cm^{-1} and the bands of 566 cm^{-1} and 445 cm^{-1} are due to Ni presence, Fe-O vibrational mode of Fe_2O_3 which attributed the hematite phase in rhombohedral lattice.

3.3 UV-Vis Analysis

Figure 3 (a) shows the absorption spectra in the UV–Vis range of Ni doped Fe2O3 nanoparticles show that all absorption curves in the range of 400–800 nm wavelengths. This result is consistent with data from other studies . Although a quantum confinement could be expected due to the decrease of the particle size upon doping, a small decrease of the absorption edge similar to the one observed in Ni in Fe_2O_3. Optical properties were observed by UV–Vis spectroscopy figure 3(b) demonstrates the optical absorption spectra of Ni doped Fe_2O_3 nanoparticles. Hematite has a direct band gap (n = 2) . UV-Visible absorption spectroscopy is one of the important tools to probe the energy band gap of the nanoparticles is calculated from

$$\mathbf{E=hc/\lambda}$$

where , E is the Band gap energy, h be the Plank's constant and c is the velocity of light , λ is wavelength of absorption edge.

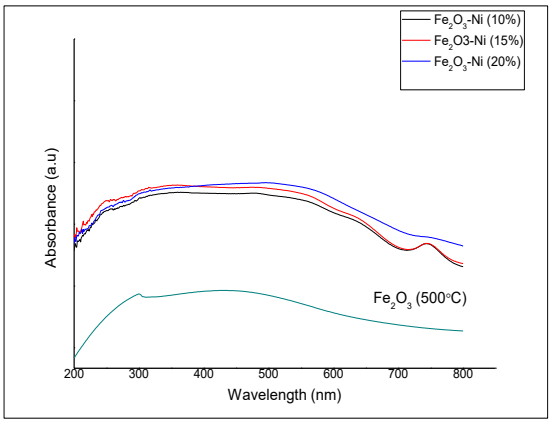

Fig.3(a): Absorbance of Fe_2O_3 & Ni doped Fe_2O_3

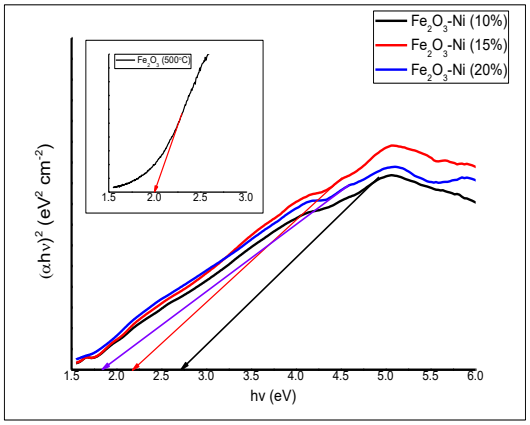

Fig.3(b): Bandgap of Fe_2O_3 & Ni doped Fe_2O_3

To calculate value of α by using the formula

$$\alpha=(2.303*A)/t$$

where, α is absoption coefficient, A is absorbance coefficient of UV-Vis spectroscopy .Then, we have calculated hν

$$\nu=c/\lambda$$

the plotted graph between $(\alpha h\nu)^{1/2}$ on y-axis and (hν) on x-axis and the value obtained is desired value of the optical band gap. Ni-doped Fe_2O_3 nanoparticles showed an optical band gap decrease from 2.4 to 1.8 eV when the nickel concentration increased up to 20 %.

3.4 Morphology SEM Analysis

Fig. 4 Shows the SEM particles has agglomated spherical -like shape with the 46 to 300nm. The surface of the nanoparticles is obtained and their sizes are determined by the scanning electron microscopy (SEM). The crystalline nature of Ni doped Fe_2O_3 nanoparticles hematite exhibited fine, spherical shape and nanometric size for the different concentrated compounds. By changing concentration of Ni, the sizes of nanoparticles also change. The size of nanoparticles of Ni-doped hematite decreases when the concentration of nickel is increased.

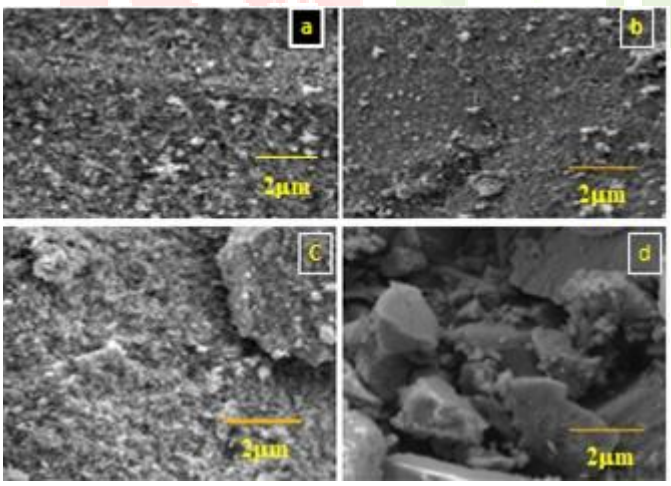

Fig.4: SEM image of (a) Fe_2O_3 (b) Ni 10% doped Fe_2O_3
(c) Ni 15% doped Fe_2O_3 (d) Ni 20% doped Fe_2O_3

Conculsion

In the present analysis, Nanocrystalline Fe_2O_3 and Ni doped Fe_2O_3 were successfully prepared by the sol gel method with different concentration of Ni (10 to 20%) and were fully Characterized by different technique. The effect of concentration change the size of particles, morphology and bandgap of the samples. From the result of XRD, FTIR, UV-Vis it confirmed formation of sample. By increasing the concentration of Ni crystalline size of doped Fe_2O_3 decreases. The FE-SEM of pure and doped samples shows the agglormated spherical in shape and the size of particle reduce. The FTIR shows the Chemical bonds formation and the optical properties analysis by UV-Vis Spectroscopy it shows the absorbance and

Optical bandgap. Ni-doped Fe_2O_3 nanoparticles showed an optical band gap decrease from 2.4 to 1.8 eV when the nickel concentration increased up to 20 %.

Acknowledgement

The author acknowledge the UGC-DAE Consortium for Scientific Research Indore-center and MNIT Jaipur for provided Characterization facility.

References

1. Shaker, S: Zafarian, C: Chakra, K:Rao, International Journal of Innovative Research in Science, Engineering and Technology, 2013,2, 2969-2973.
2. Adnan, A:Wardy, H: Ogaili, S: Abbas, International Journal of Innovative Research in Science, Engineering and Technology, 2016, 5, 5560-5567.
3. Akbar, S:Hasanain, N:Azmat, M:Nadeem
4. Cheng, A:Tan,Y: Tao, D: Shan, K:Ting, X: Yin, International Journal of Photoenergy, 2012, Article ID 608298, 5.
5. Tharani, L: Nehru, International Journal of Advanced Research in Physical Science, 2015, 2,47-50.
6. Kooti, L:Matouri, Journal of Material Science, 2014, 2, 37-42.
7. Mirzaei, K:Janghorban, B:Hashemi, S:Hosseini, M:Bonyani, S:Leonardi, A: Bonavita, G:Neri, Processing and Application of Ceramics,2016, 10 ,209–217.
8. Alagiri, S:Hamid, J Sol-Gel Sci Technol, 2015, 74, 783–789.
9. P:Mallick, Materials Science-Poland, 2014,32(2),193-197.
10. Lassoued, M:Lassoued, S:Granda, B:Dkhil, S: Ammar, A:Gadri, J Mater Sci: Mater Electron, 2018,
11. Suresh, K: Giribabu, R: Manigandan, A: Stephen,V:Narayanan, Journal of nanoscience and Technology,2015,1,1-3.
12. F:Lan, X:Wang, X:Xu, React. Kinet. Mech. Catal., 2012, 106, 113–125.
13. M:Mohammadikish, Ceram. Int.,2014, 40, 1351–1358 .